Kinase Sensing

DOI: 10.1002/ange.201408256

Differential Sensing of MAP Kinases Using SOX-Peptides**

Diana Zamora-Olivares, Tamer S. Kaoud, Jiney Jose, Andrew Ellington, Kevin N. Dalby, and Eric V. Anslyn**

Abstract: *Five SOX peptides are used to classify the MAPK groups and isoforms thereof using chemometrics. The score plots show excellent classification and accuracy, while support vector machine analysis leads to the quantification of ERK and an ERK inhibitor concentration in kinase mixtures. Examination of the loading plots reveals cross-reactivity among the peptides, and some unexpected surprises.*

Mitogen-activated protein kinases (MAPKs) are key regulators of cellular processes, and their aberrant activity is associated with several diseases: cancer, diabetes, and neurodegenerative and hematological malignances.[1] MAPKs are classified in three major groups, the extracellular signal regulated kinases (ERK1/2), the c-jun N-terminal kinases (JNK1/2/3), and the p38 MAPKs (p38α/β/γ/δ). Conventional detection methods for these groups, and their isoforms, rely either on the use of radioassays or antibodies.[2] More recently, optical-based biosensors have emerged to detect kinase activity.[3] For instance, the peptide-based sensors developed by the Imperiali group, containing a sulfonamidooxine (SOX) fluorophore, is a leading approach. Upon peptide phosphorylation proximal to SOX, this fluorophore increases its affinity for Mg^{2+}, resulting in chelation-enhanced fluorescence.[4] Imparting selectivity to the biosensors for distinguishing between kinases is a challenge, and is achieved by varying the peptide structure.[5]

[*] Dr. D. Zamora-Olivares, Prof. E. V. Anslyn
Department of Chemistry and Biochemistry
The University of Texas at Austin
1 University Station A1590, Austin, Texas 78712 (USA)
E-mail: anslyn@austin.utexas.edu
Dr. T. S. Kaoud, Prof. K. N. Dalby
Division of Medicinal Chemistry
The University of Texas at Austin
1 University Station A1590, Austin, Texas 78712 (USA)
E-mail: kinases@me.com
Prof. A. Ellington
Institute for Cell and Molecular Biology
The University of Texas at Austin
Dr. J. Jose
Faculty of Medical and Health Sciences
University of Auckland, Auckland, 92019 (New Zealand)

[**] We gratefully acknowledge support for this work from the Welch Foundation (F-1151 and F-1390), NSF (CHE-1212971), and NIH (GM059802 and CA167505). D.Z.O. acknowledges a CONACYT fellowship (212537). T.S.K. acknowledges a Cancer Prevention and Research Institute of Texas Postdoctoral Training Award (RP101501). We thank Dr. Pavel Anzenbacher and Dr. Nina Esipenko for their advice and insight. MAP kinases = mitogen-activated protein kinases.

Supporting information for this article is available on the WWW under http://dx.doi.org/10.1002/anie.201408256.

The design of the peptides that control selectivity relies on differences between the recruitment sites of MAPKs.[6] These sites control the specificity of the kinase docking interactions with upstream activators, phosphatases, and downstream substrates.[7] Two different MAPK recruitment sites have been identified, the D-recruitment site (DRS) and the F-recruitment site (FRS), which recognize modular peptide sequences in their substrates.[8] Some MAPKs, such as the ERKs possess both, while others, such as the JNKs are believed to possess only a DRS. By targeting these sites a selective SOX-peptide was synthesized to study the activity of p38α,[9] while a different SOX-peptide, with different recognition elements, exhibited selectivity for ERK1/2.[10] In such a strategy, one designs a different SOX-peptide for each kinase target.

In contrast, the differential sensing method enables the detection of closely related analytes by using an array of cross-reactive receptors, creating a response pattern that is diagnostic for individual targets or mixtures.[11] Our group,[12] and others,[13] have used this pattern recognition approach for the differentiation of proteins. Recently, we reported the in situ formation of an array of Zn^{II} dipicolylamine chemosensors targeted to kinases. Seven different hosts were used to classify phosphorylation stages of MAPKs, as well as to differentiate cell extracts of varying kinase expression.[14] Herein, we report an alternative differential sensing strategy for kinases. The approach uses five SOX-peptides with distinctive docking sites for MAPKs, and shows considerably higher sensitivity and better cross-reactivity than the previous approach. This array was used to qualitatively differentiate each of the following: ERK1/2, JNK1/2/3, and p38α/β/δ/γ. In addition, changes of kinase concentration, as well as specific inhibitor concentration, were quantitatively detected in kinase mixtures. Further, the chemometric results revealed unexpected cross-reactivity of the SOX-peptides, and interdependences between the kinases that otherwise would not necessarily be evident.

We chose peptides with differing selectivities for MAPKs based upon previously reported results. In addition, we adopted the fluorescence sensing strategy reported by the Imperiali group, in which the Cys residue at the P+2 or P−2 position in each peptide was functionalized with the SOX fluorophore, yielding the fluorescent docking peptides: SOX-Sub-D (**1a**), SOX-MEF2A (**1b**), SOX-NFAT4 (**1c**), SOX-Sub-F (**1d**) and SOX-p38 (**1e**) (Figure 1). The first and fourth peptides were designed based on a report by Dalby, where he found that the Sub-D and Sub-F peptides bind to the DRS and the FRS of ERK2, respectively.[15] The DRS exists in ERK, JNK, and p38 MAPKs.[16] Thus, it was expected that Sub-D will be phosphorylated by any of these kinases. In contrast, the FRS has been found primarily in ERK and p38α,

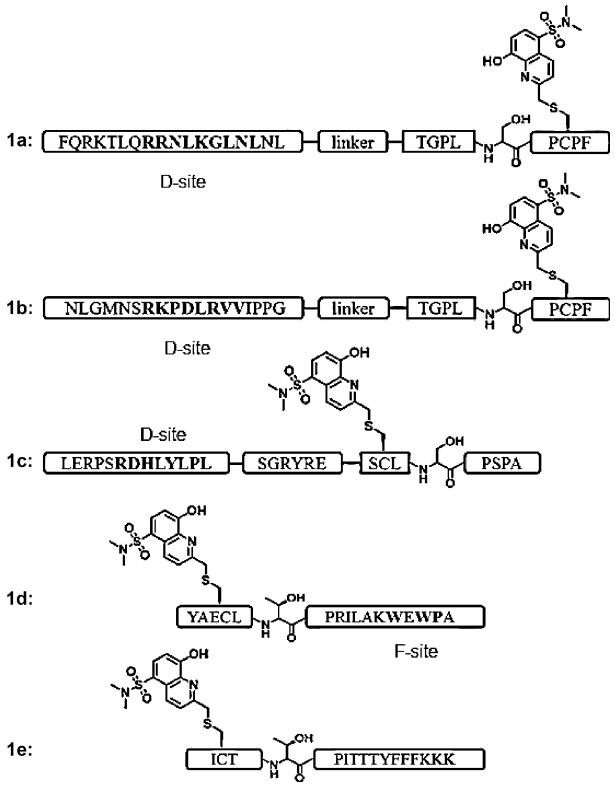

Figure 1. Peptide-based sensing array. SOX-peptide substrates presenting docking sites for MAPK recognition. Linker = three 6-aminohexanoic acid groups.

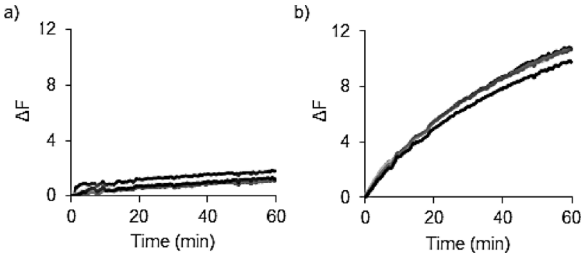

Figure 2. Fluorescence changes of SOX-NFAT4 peptide upon phosphorylation with different MAPKs, showing four experimental replicates. Enzymatic activity of a) ERK1 and b) JNK2 with SOX-NFAT4 peptide (2 μM).

but not in p38β or JNKs;[17] for this reason Sub-F affinity was expected towards ERKs and some p38 isoforms.[18] The second and third peptides were reported by Garai et al. He found that the docking peptide derived from MEF2A (myocyte enhancer factor 2A) bound ERK2 and p38α, while a peptide derived from NFAT4 (nuclear factor of activated T cells 4) bound to JNK1.[19] Because the MEF2A-derived peptide previously used is very long,[19] only the D-motif was retained, and linked by means of 6-aminohexanoic acid to the phosphorylation motif. Further, the phosphorylation motif TPVVSVTTPS was replaced with TGPLSPCPF because Dalby and Turk had reported that this motif is relatively nonspecific, and differential sensing benefits from cross-reactivity.[18] Lastly, Chen et al., found that the p38 peptide shows good selectivity for the p38 group, having highest affinity to p38α,[20] Therefore, addition of peptide **1e** to our array was expected to assist in the classification of these kinases.

We first sought to challenge the discriminatory power of our cross-reactive peptides to distinguish nanomolar levels of the MAPK isoforms: ERK1/2 (0.5 nM), JNK1/2/3 (5 nM), and p38α/β/γ/δ (2.5 nM), with each SOX-peptide at 2 μM, with the exception of SOX-p38 peptide (8 μM). Kinetics traces for SOX-peptide phosphorylation by each kinase were recorded for 60 min in four replicates (Figure 2 shows two representative examples, see the Supporting Information for all data). The delta fluorescence (ΔF) values at 20 min, along with calculated rate constants,[21] were used as input for chemometric analysis (Supporting Information).

The multivariate data (4 replicates × 5 peptides × 9 kinases × 2 inputs) were analyzed with the program XLSTAT using both principal component analysis (PCA) and linear discriminant analysis (LDA). PCA is an unsupervised method, which is used to find the greatest variance in the data set without any predetermined bias for classification. In contrast, LDA maximizes the separation between known differing classes, while minimizing the scatter within each analyte class.[22] Thus, for the classification of known kinase groups and isoforms, as well as concentrations (vide infra) we turned to LDA. The score plot (Figure 3a, a 2D representation is in the Supporting

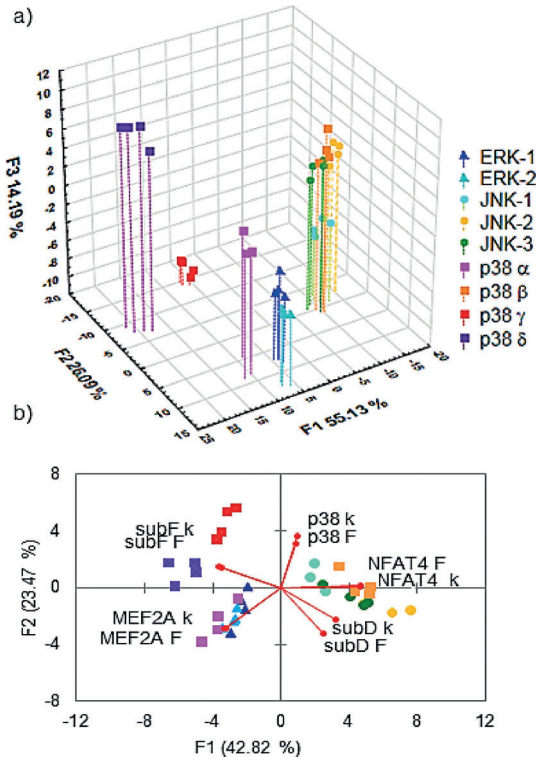

Figure 3. Fingerprints of the MAPKs produced by the peptidic array. a) Three-dimensional LDA plot of the response from the SOX-peptides showing in vitro differentiation of nine MAP kinases. b) PCA biplot showing the peptide contributions to the differentiation of the MAPKs. $F = \Delta F$ at 20 min, k = rate constant.

Information) was obtained with 94.4% classification accuracy according to a jack-knife analysis. LDA successfully differentiated and categorized the MAPK isoforms into their three corresponding groups, with the exception of p38β, which was unexpectedly found in close proximity to the JNK group.

To reveal which SOX-peptides led to differentiation of the kinases we used PCA. Although more scatter is common with PCA, the unbiased nature of the plot makes it superior for revealing which variables (peptides in this study) lead to classification of the groups (kinases). To visualize the dependence between the variables and groups, loading plots are used. In our study the direction and magnitude of the discriminate vectors in the PCA loading plot show the extent to which the peptides contribute to the discrimination of the kinases along the factor axes of the score plot. Biplots superimpose the score and loading plots to readily reveal which discriminate vectors correlate with group classification (Figure 3b).[22a]

The discriminate vectors in the biplot were found to support the aforementioned literature results for phosphorylation selectivities, but some unexpected cross-reactivity was uncovered. For instance, the MEF2A vector indeed correlates well with ERK2 and p38α, but also with ERK1 and even p38δ to some extent. Further, as expected, the NFAT4 discriminate vector indicates that this peptide was phosphorylated by JNK1, but it actually shows a greater contribution to differentiating the other JNK group members, as well as p38β. Further, although the p38 peptide was mainly phosphorylated by the p38 kinase group as expected, the discriminate vectors show that this peptide primarily differentiates only the p38γ and p38δ isoforms from the other kinases. As expected, Sub-F was phosphorylated by the ERKs and most p38 isoforms due to binding to the FRS. The kinetics revealed that the p38 group phosphorylated this peptide with higher efficiency. Thus, the Sub-F discriminate vectors mainly contributed to the discrimination of ERKs, as well as p38α, p38γ, and p38δ. Lastly, Sub-D was expected to be phosphorylated by most MAPKs, and thus would be quite cross-reactive and beneficial to the analysis. Indeed, Sub-D was the least selective peptide, but because its discriminate vectors lie nearly equally between the ERK and JNK groups, the response to this peptide contributes to the discrimination of these groups the most. In summary, when the composite response from the array is analyzed using chemometrics, the peptides were found to be cross-reactive and not necessarily highly selective for their predicted individual kinases. Hence, a differential sensing approach has considerable power in classifying the MAPK groups, and also their isoforms, in one in vitro assay.

Next, we explored whether the array could be used to quantitatively determine the concentration of a kinase in a mixture of kinases. Thus, a study was performed in which the concentrations of ERK1 were increased in the presence of fixed concentrations of JNK3 and p38γ (Figure 4a). In this case, as well as the next study, LDA was used because the goal was to make a clear classification of concentrations. The LDA plot revealed a curved dependence of the intergroup variance along the F1 and F2 axes. In such cases, Anzenbacher has introduced the use of support vector machines (SVMs) for quantitative data analysis in differential sensing.[23] SVMs are used to analyze datasets of numerical classes with nonlinear

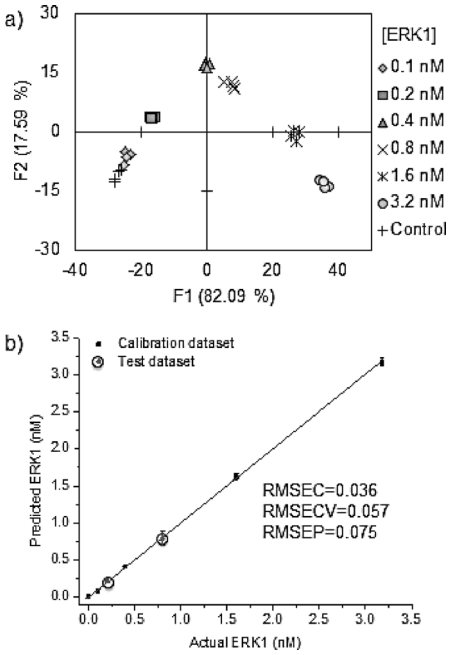

Figure 4. Results of the quantitative analysis of ERK1 in the presence of JNK3 (5 nM) and p38γ (2.5 nM) MAPKs. a) LDA plot showing the response of the SOX-peptides to the in vitro differentiation of ERK1 concentration. b) Results of the SVM regression method for ERK1 in a mixture of kinases. The unknown samples (circled dots) were correctly analyzed. The root-mean-square errors (RMSEs) of calibration (C), cross-validation (CV), and prediction (P) indicate the accuracy of the model and prediction.

behavior. These classes are rearranged into a higher-dimensional vector space using kernel functions.[24] The SVM regression method constructs calibration models which predict the properties (concentrations in our studies) of unknown samples.[25] Thus, a SVM model was used for regression analysis of ERK1 in MAPK mixtures. The acquired multivariate data was divided into two sets: one to generate the calibration model and the second to validate the model. For ERK analysis, two concentrations of seven (29% of the data) were analyzed as unknown concentrations, and the calibration model was used to calculate the unknown samples. This peptide array yielded an accurate quantitative determination of ERK1, where the unknown concentrations were correctly quantified (dots) as shown in Figure 4b. The test model used to validate the calibration model produces a root-mean-square error of prediction (RMSEP) value, which gives a measure of the predictive performance of the calibration model when presented with unknown data. An error of only 2.4% was obtained according to the RMSEP = 0.075.

Finally, we set out to explore whether the cross-reactive peptides could be used to analyze kinase inhibitor activity. A variety of small-molecule inhibitors have been developed to regulate the activity of the ERK pathway.[26] However, few detection methods have been developed that are amenable to screening the in vitro activity of inhibitors using mixtures. To explore the utility of this sensing ensemble for monitoring inhibitors, a kinase assay with the specific ERK inhibitor VX-11e[27] was investigated to fingerprint the inhibition of ERK1

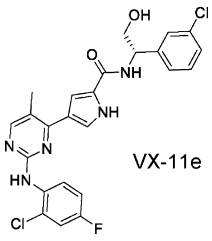

in the presence of JNK3 and p38γ. The resulting LDA score plot (Figure 5a) presented a slightly curved progression of the data primarily along F1. The kinetics showed that MEF2A presented a significant decrease in the fluorescence intensity, whereas a moderate fluorescence decrease was observed with Sub-F peptide at low

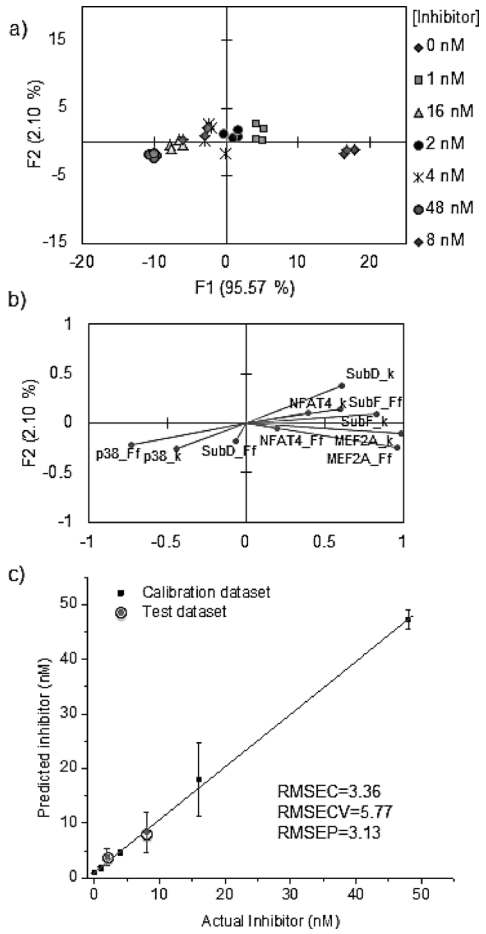

Figure 5. Results of the chemometric analysis of inhibitor VX-11e in the presence of ERK1 (0.5 nM), JNK3 (5 nM), and p38γ (2.5 nM) kinase mixture. a) LDA score plot and b) loading plot showing the response of the SOX-peptides to different inhibitor concentrations. c) Results of quantitative analysis of inhibitor in a mixture of kinases. The prediction plot and root-mean-square errors (RMSEs) indicate the accuracy of the calibration model and test validation.

inhibitor concentrations. Thus, the MEF2A and Sub-F vectors in the loading plot (Figure 5b) contributed to the differentiation of low inhibitor concentrations. Interestingly, however, an otherwise unanticipated dependence of the p38 peptide on the ERK inhibitor concentration was revealed, showing a moderate increase in the kinetic activity with increasing ERK inhibitor concentration. The loading vectors show that this increase in activity contributes to differentiation of the high inhibitor concentrations. In fact, p38 and ERK are reported to form a heterodimer that inhibits their activities.[28] Therefore, our hypothesis is that VTX-11e activates p38 by promoting its release from this inhibitory heterodimer. Such unanticipated results in inhibitor behavior can only be revealed with a parallel analysis of peptide cross-reactivity with mixtures of kinases, and examination of loading plots, as is inherent in a differential sensing routine.

Overlap of data clusters was observed at low inhibitor concentrations, yielding lower classification accuracy than with ERK concentration. However, despite this overlap at low concentrations, a trend was observed showing a dependence of the response on increasing inhibitor concentrations. As with the ERK concentration studies, for the analysis of the ERK-inhibitor, we used five concentrations to build the calibration model using a SVM regression method. Two concentrations were used as unknowns for cross-validation. The regression analysis of inhibitor concentrations allowed for the correct prediction of the unknowns (circles) in Figure 5c. The RMSEP yielded a 6.6% error of the predictive accuracy of the model.

In summary, this study showed that the discriminating properties of the docking sites on MAPK substrates can be used to develop a pattern recognition approach for fingerprinting kinases. Nine MAPK isoforms were classified by using this differential sensing approach. The use of a PCA biplot revealed the cross-reactivity of the peptides, and their respective contributions to the kinase classification. Furthermore, this array allowed for the quantitative analysis of ERK1 and inhibitor concentrations in mixtures of kinases. From these results, SOX-peptides proved to be excellent choices for a differential sensing approach that relies on a significant extent of cross-reactivity. Importantly, by performing a chemometric analysis of the SOX-peptide substrate activities, their respective contributions to classifying kinases, as well as kinase and inhibitor concentrations, can be tested or discovered, and unexpected trends in reactivity revealed.

Received: August 15, 2014
Published online: October 15, 2014

Keywords: biosensors · chemometrics · differential sensing · fluorescent probes · mitogen-activated protein kinases

[1] G. Manning, D. B. Whyte, R. Martinez, T. Hunter, S. Sudarsanam, *Science* **2002**, *298*, 1912–1934.
[2] a) L. Bonetta, *Nat. Methods* **2005**, *2*, 225–232; b) K. A. Janes, J. G. Albeck, L. X. Peng, P. K. Sorger, D. A. Lauffenburger, M. B. Yaffe, *Mol. Cell. Proteomics* **2003**, *2*, 463–473; c) J. Rush, A. Moritz, K. A. Lee, A. Guo, V. L. Goss, E. J. Spek, H. Zhang, X.-M. Zha, R. D. Polakiewicz, M. J. Comb, *Nat. Biotechnol.* **2005**, *23*, 94–101.
[3] a) C. Prével, M. Pellerano, T. N. N. Van, M. C. Morris, *Biotechnol. J.* **2014**, *9*, 253–265; b) J. A. González-Vera, *Chem. Soc. Rev.* **2012**, *41*, 1652–1664.
[4] M. D. Shults, K. A. Janes, D. A. Lauffenburger, B. Imperiali, *Nat. Methods* **2005**, *2*, 277–284.
[5] C. I. Stains, N. C. Tedford, T. C. Walkup, E. Luković, B. N. Goguen, L. G. Griffith, D. A. Lauffenburger, B. Imperiali, *Chem. Biol.* **2012**, *19*, 210–217.

[6] T. S. Kaoud, S. Mitra, S. Lee, J. Taliaferro, M. Cantrell, K. D. Linse, C. L. Van Den Berg, K. N. Dalby, *ACS Chem. Biol.* **2011**, *6*, 658 – 666.

[7] R. Akella, T. M. Moon, E. J. Goldsmith, *Biochim. Biophys. Acta Proteins Proteomics* **2008**, *1784*, 48 – 55.

[8] T. Lee, A. N. Hoofnagle, Y. Kabuyama, J. Stroud, X. Min, E. J. Goldsmith, L. Chen, K. A. Resing, N. G. Ahn, *Mol. Cell* **2004**, *14*, 43 – 55.

[9] C. I. Stains, E. Luković, B. Imperiali, *ACS Chem. Biol.* **2010**, *6*, 101 – 105.

[10] E. Luković, E. Vogel Taylor, B. Imperiali, *Angew. Chem. Int. Ed.* **2009**, *48*, 6828 – 6831; *Angew. Chem.* **2009**, *121*, 6960 – 6963.

[11] E. V. Anslyn, *J. Org. Chem.* **2007**, *72*, 687 – 699.

[12] A. T. Wright, M. J. Griffin, Z. Zhong, S. C. McCleskey, E. V. Anslyn, J. T. McDevitt, *Angew. Chem. Int. Ed.* **2005**, *44*, 6375 – 6378; *Angew. Chem.* **2005**, *117*, 6533 – 6536.

[13] a) L. Motiei, Z. Pode, A. Koganitsky, D. Margulies, *Angew. Chem. Int. Ed.* **2014**, *126*, 9289 – 9293; *Angew. Chem.* **2014**, *53*, 9443 – 9447; b) H. Kong, Y. Lu, H. Wang, F. Wen, S. Zhang, X. Zhang, *Anal. Chem.* **2012**, *84*, 4258 – 4261; c) P. Wu, L.-N. Miao, H.-F. Wang, X.-G. Shao, X.-P. Yan, *Angew. Chem. Int. Ed.* **2011**, *50*, 8118 – 8121; *Angew. Chem.* **2011**, *123*, 8268 – 8271; d) X. Li, F. Wen, B. Creran, Y. Jeong, X. Zhang, V. M. Rotello, *Small* **2012**, *8*, 3589 – 3592; e) D. F. Moyano, S. Rana, U. H. F. Bunz, V. M. Rotello, *Faraday Discuss.* **2011**, *152*, 33 – 42; f) O. R. Miranda, H.-T. Chen, C.-C. You, D. E. Mortenson, X.-C. Yang, U. H. F. Bunz, V. M. Rotello, *J. Am. Chem. Soc.* **2010**, *132*, 5285 – 5289; g) M. De, S. Rana, H. Akpinar, O. R. Miranda, R. R. Arvizo, U. H. F. Bunz, V. M. Rotello, *Nat. Chem.* **2009**, *1*, 461 – 465; h) C.-C. You, O. R. Miranda, B. Gider, P. S. Ghosh, I.-B. Kim, B. Erdogan, S. A. Krovi, U. H. F. Bunz, V. M. Rotello, *Nat. Nanotechnol.* **2007**, *2*, 318 – 323; i) D. Margulies, A. D. Hamilton, *Angew. Chem. Int. Ed.* **2009**, *48*, 1771 – 1774; *Angew. Chem.* **2009**, *121*, 1803 – 1806; j) H. Zhou, L. Baldini, J. Hong, A. J. Wilson, A. D. Hamilton, *J. Am. Chem. Soc.* **2006**, *128*, 2421 – 2425; k) S. Kolusheva, R. Zadmard, T. Schrader, R. Jelinek, *J. Am. Chem. Soc.* **2006**, *128*, 13592 – 13598.

[14] D. Zamora-Olivares, T. S. Kaoud, K. N. Dalby, E. V. Anslyn, *J. Am. Chem. Soc.* **2013**, *135*, 14814 – 14820.

[15] S. Lee, M. Warthaka, C. Yan, T. S. Kaoud, P. Ren, K. N. Dalby, *Biochemistry* **2011**, *50*, 9500 – 9510.

[16] S. Liu, J.-P. Sun, B. Zhou, Z.-Y. Zhang, *Proc. Natl. Acad. Sci. USA* **2006**, *103*, 5326 – 5331.

[17] a) A. Galanis, S.-H. Yang, A. D. Sharrocks, *J. Biol. Chem.* **2001**, *276*, 965 – 973; b) N. Tzarum, N. Komornik, D. Ben Chetrit, D. Engelberg, O. Livnah, *J. Biol. Chem.* **2013**, *288*, 19537 – 19547.

[18] D. L. Sheridan, Y. Kong, S. A. Parker, K. N. Dalby, B. E. Turk, *J. Biol. Chem.* **2008**, *283*, 19511 – 19520.

[19] A. Garai, A. Zeke, G. Gogl, I. Toro, F. Fordos, H. Blankenburg, T. Barkai, J. Varga, A. Alexa, D. Emig, M. Albrecht, A. Remenyi, *Sci. Signaling* **2012**, *5*, ra74.

[20] G. Chen, M. D. Porter, J. R. Bristol, M. J. Fitzgibbon, S. Pazhanisamy, *Biochemistry* **2000**, *39*, 2079 – 2087.

[21] A. K. Devkota, T. S. Kaoud, M. Warthaka, K. N. Dalby, *Curr. Protoc. Mol. Biol.* **2010**, *Chapter 18*, Unit 18.17.

[22] a) S. Stewart, M. A. Ivy, E. V. Anslyn, *Chem. Soc. Rev.* **2014**, *43*, 70 – 84; b) P. Anzenbacher, M. A. Palacios, *Chemosensors*, Wiley, Hoboken, **2011**, pp. 345 – 368.

[23] T. Minami, N. A. Esipenko, A. Akdeniz, B. Zhang, L. Isaacs, P. Anzenbacher, *J. Am. Chem. Soc.* **2013**, *135*, 15238 – 15243.

[24] L. Hamel, *Knowledge Discovery with Support Vector Machines*, Wiley, Hoboken, **2009**, pp. 89 – 132.

[25] R. G. Brereton, *Chemometrics for Pattern Recognition*, Wiley, Hoboken, **2009**, pp. 47 – 106.

[26] J. L. Yap, S. Worlikar, A. D. MacKerell, P. Shapiro, S. Fletcher, *ChemMedChem* **2011**, *6*, 38 – 48.

[27] A. M. Aronov, Q. Tang, G. Martinez-Botella, G. W. Bemis, J. Cao, G. Chen, N. P. Ewing, P. J. Ford, U. A. Germann, J. Green, M. R. Hale, M. Jacobs, J. W. Janetka, F. Maltais, W. Markland, M. N. Namchuk, S. Nanthakumar, S. Poondru, J. Straub, E. ter Haar, X. Xie, *J. Med. Chem.* **2009**, *52*, 6362 – 6368.

[28] a) H. Zhang, X. Shi, M. Hampong, L. Blanis, S. Pelech, *J. Biol. Chem.* **2001**, *276*, 6905 – 6908; b) V. Sanz-Moreno, B. Casar, P. Crespo, *Mol. Cell. Biol.* **2003**, *23*, 3079 – 3090.

